

# GHz Bandstop Microstrip Filter Using Patterned $\text{Ni}_{78}\text{Fe}_{22}$ Ferromagnetic Film

Y. Zhuang, B. Rejaei, E. Boellaard, M. Vroubel, and J. N. Burghartz

**Abstract**—A series of microstrips with patterned  $\text{Ni}_{78}\text{Fe}_{22}$  ferromagnetic cores have been investigated for RF applications. The devices have been integrated onto a silicon substrate by using a fully IC-compatible process. The  $\text{Ni}_{78}\text{Fe}_{22}$  films were deposited by electroplating onto Si at room temperature and were structured into rectangular prisms with large aspect ratios, i.e., 10:1 and 40:1. Measurements have been performed using a network analyzer. Voltage attenuation of 19 dB/cm has been obtained at 3.9 GHz on a 2-mm-long strip line. The propagating wavelength is reduced by 60% compared to a control device without ferromagnetic core.

**Index Terms**—Microstrip, on-chip, permalloy, radio frequency (RF), soft magnetic materials.

## I. INTRODUCTION

INTEGRATION of microstrip devices with ferromagnetic materials has recently attracted considerable attention for radio frequency (RF) applications, e.g., stopband filters and quarter wavelength strip lines. The stopband filter relies on energy absorption by ferromagnetic resonance (FMR) and its center stopband frequency is determined by FMR frequency. For the quarter wavelength strip line, the size of the device can be reduced considerably due to the large wavelength shortening caused by ferromagnetic (FM) films. In both cases, the use of magnetic materials with high permeability at high operating frequencies is essential for satisfactory performance. In [1]–[3], single crystalline Fe films have been grown on a GaAs substrate using molecular beam epitaxy (MBE). High attenuation of 50 dB/cm has been reported on a notch filter [4]. However, MBE growth is incompatible with the standard Si integrated circuit (IC) technologies. Few works have addressed other ferromagnetic materials [5], [6]. Permalloy (NiFe), on the other hand, has an overall advantage, because it has been intensively studied and is widely used in industry [7]–[9]. However, the low saturation magnetization ( $\sim 1$  Tesla) and the low FMR frequency ( $\sim 0.1$  GHz) limit its RF applications.

In this letter, a series of microstrip devices with electroplated permalloy  $\text{Ni}_{78}\text{Fe}_{22}$  films on a silicon substrate are investigated. We present a method to utilize plated permalloy  $\text{Ni}_{78}\text{Fe}_{22}$  films at frequencies above 1 GHz by means of micro-patterning. The films are then used to realize microstrips on silicon substrates

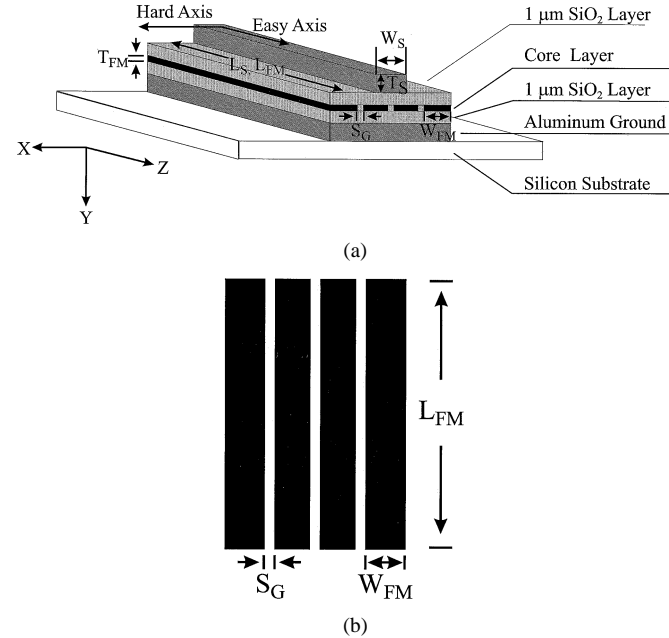


Fig. 1. (a) Schematic illustration of the microstrip line structure. The core layer is i) one prism of  $\text{Ni}_{78}\text{Fe}_{22}$  with dimension  $2000 \times 200 \times 0.5 \mu\text{m}$ , ii) four parallel prisms of  $\text{Ni}_{78}\text{Fe}_{22}$  with dimension for each prism  $2000 \times 50 \times 0.5 \mu\text{m}$ , and iii) one prism of  $\text{SiO}_2$  with dimension  $2000 \times 200 \times 0.5 \mu\text{m}$ , for sample #A, #B, #Ref, respectively. (b) Top view of a patterned  $\text{Ni}_{78}\text{Fe}_{22}$  core.

with a short wavelength, high attenuation, and high center stopband frequency.

## II. EXPERIMENT

Microstrip transmission lines with 0.5-μm-thick  $\text{Ni}_{78}\text{Fe}_{22}$  core have been integrated on a silicon wafer using a fully IC compatible process. A schematic drawing of the device is shown in Fig. 1. The  $\text{Ni}_{78}\text{Fe}_{22}$  films were electroplated under a dc magnetic field 64 kA/m applied along the easy axis at room temperature. The prism-like patterns of the  $\text{Ni}_{78}\text{Fe}_{22}$  films were defined in photoresist by conventional lithography and were formed by through-resist-plating. Three types of samples are presented in this work, with their detailed structural parameters listed in Table I. The aspect ratio ( $L_{FM} : W_{FM}$ ) of the ferromagnetic prism is 10:1 for sample #A, and 40:1 for each of the four prisms of #B. Sample #Ref is a controlled device with the same geometrical parameters as samples #A and #B, but using a 0.5-μm-thick dielectric  $\text{SiO}_2$  film instead of the  $\text{Ni}_{78}\text{Fe}_{22}$  film.

The magnetic properties of the  $\text{Ni}_{78}\text{Fe}_{22}$  films were characterized by means of magneto-optical Kerr effect (MOKE) and vibrating sample magnetometry (VSM) measurements.

Manuscript received March 25, 2002; revised June 26, 2002. This work was supported by the Foundation for Fundamental Research on Matter (FOM), the Netherlands. The review of this letter was arranged by Associate Editor Dr. Arvind Sharma.

The authors are with the Laboratory of Electronic Components, Technology, and Materials, Delft Institute of Microelectronics and Submicron technology, Delft University of Technology, Delft, The Netherlands.

Digital Object Identifier 10.1109/LMWC.2002.805934

TABLE I

STRUCTURAL PARAMETERS OF STRIPS #A, #B AND #REF.  $T_S$ ,  $W_S$ , AND  $L_S$  ARE THE THICKNESS, WIDTH, AND LENGTH OF THE METAL STRIP;  $T_{FM}$ ,  $W_{FM}$ , AND  $L_{FM}$  ARE THE THICKNESS, WIDTH, AND LENGTH OF THE FERROMAGNETIC FILMS, RESPECTIVELY.  $N$  IS THE NUMBER OF PATTERNED FERROMAGNETIC PRISMS, AND  $S_G$  IS THE GAP OF THE ADJACENT PRISMS

	Metal Strip (aluminum)			Core Layer					
	$T_S$ ( $\mu\text{m}$ )	$W_S$ ( $\mu\text{m}$ )	$L_S$ ( $\mu\text{m}$ )	Material	$T_{FM}$ ( $\mu\text{m}$ )	$W_{FM}$ ( $\mu\text{m}$ )	$L_{FM}$ ( $\mu\text{m}$ )	$N$	$S_G$ ( $\mu\text{m}$ )
#A	3.0	50.0	2000.0	$\text{Ni}_{78}\text{Fe}_{22}$	0.5	200.0	2000.0	1	-----
#B	3.0	50.0	2000.0	$\text{Ni}_{78}\text{Fe}_{22}$	0.5	50.0	2000.0	4	5.0
#Ref	3.0	50.0	2000.0	$\text{SiO}_2$	0.5	200.0	2000.0	1	-----

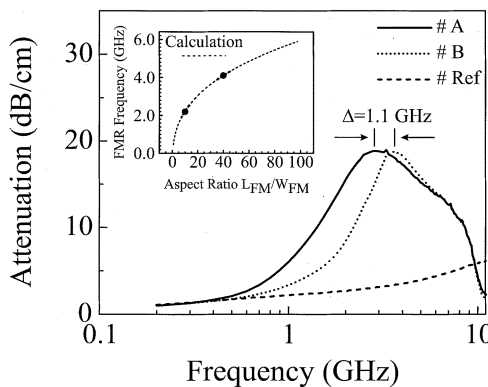


Fig. 2. Attenuation per unit length as function of frequency. The inset plots the dependency of the calculated ferromagnetic resonance frequency versus shape aspect ratio of FM patterning. The two solid circles correspond to the experiment with the same shape aspect ratio.

The magnetocrystalline anisotropy  $\mu_0 H_{am}$  of the  $\text{Ni}_{78}\text{Fe}_{22}$  films is about 0.6 mT, where  $\mu_0$  is the permeability of vacuum. Characterizations of the devices were performed on a HP-8510 network analyzer, using a ground–signal–ground (G–S–G) two-port configuration.

### III. RESULTS AND DISCUSSION

Attenuation constant  $\alpha$  measured on samples #A, #B with 0.5  $\mu\text{m}$   $\text{Ni}_{78}\text{Fe}_{22}$  film, and on the control sample #Ref without ferromagnetic core, is shown in Fig. 2. Since there is no attenuation peak observed on #Ref up to 11 GHz, the attenuation peaks observed on both #A and #B are due to the presence of ferromagnetic resonance of the  $\text{Ni}_{78}\text{Fe}_{22}$  film. Despite the different patterning of the FM films, an equal attenuation of about 19 dB/cm (in voltage) has been obtained for both #A and #B. The center stopband frequency reaches 2.8 GHz for #A and 3.9 GHz for #B. The observed high stopband frequencies are a result of the high aspect ratios, and, hence, the large shape anisotropy of the patterned  $\text{Ni}_{78}\text{Fe}_{22}$  films. In general, the resonance frequency  $\omega_r$  of a saturated FM film is given by [10]

$$\omega_r = \{[\omega_0 + \omega_{am} + (N_x - N_z)\omega_M] \cdot [\omega_0 + \omega_{am} + (N_y - N_z)\omega_M]^{1/2} \quad (1)$$

where  $\omega_0 = \gamma\mu_0 H_0$ ,  $\omega_{am} = \gamma\mu_0 H_{am}$ ,  $\omega_M = \gamma M_0$ , and  $\gamma$  is the gyromagnetic constant (176 GHz/T), and  $H_0$ ,  $H_{am}$ , and  $M_0$  denote, respectively, the applied dc field, magnetocrystalline

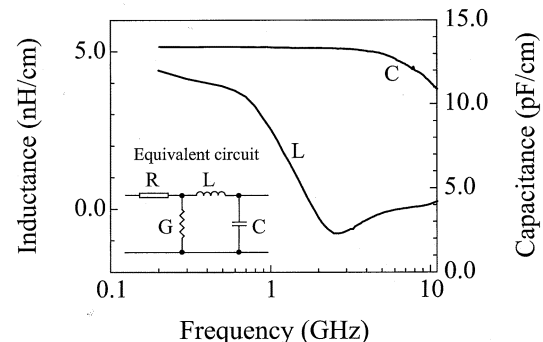


Fig. 3. Dependence of inductance ( $L$ ) and capacitance ( $C$ ) per unit length versus the frequency on sample #A. The inset shows the equivalent circuit of a microstrip structure.  $R$  and  $G$  denote the series resistance and shunt conductance per unit length, respectively.

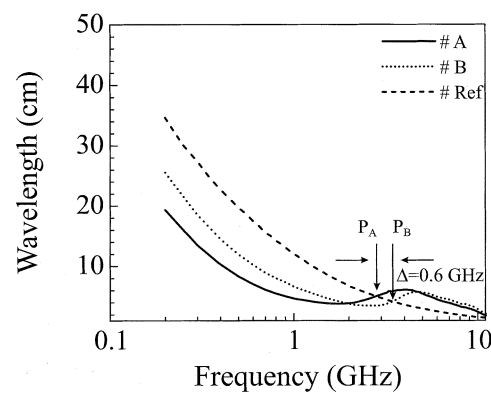


Fig. 4. Propagation wavelength as function of frequency.  $P_A$  and  $P_B$  denote the frequencies at which the propagation wavelength in samples #A and #B is equal to that in the control sample #Ref, respectively.  $\Delta$  represents the frequency shift between  $P_A$  and  $P_B$ .

anisotropy field, and the saturation magnetization. The demagnetizing factors  $N_x$ ,  $N_y$ , and  $N_z$  are determined by the shape of the FM patterns. For rectangular prisms,  $N_x$ ,  $N_y$ , and  $N_z$  are expressed as sums of a series of tangent functions [11], where their mean values are obtained by averaging over the whole FM film [12]. The FMR frequencies are calculated as a function of the aspect ratio  $L_{FM}/W_{FM}$ , and the results are displayed in the inset of Fig. 2 using a saturation magnetization and a damping factor of the  $\text{Ni}_{78}\text{Fe}_{22}$  film 1.04 Tesla and 0.05, respectively. It turns out that a higher shape aspect ratio leads to a higher FMR frequency. The frequency shift between the two solid circles (the same aspect ratios as the experiment, 10:1 and 40:1, respectively) is in a good agreement with the experimental results.

The influence of ferromagnetic film on the lumped circuit parameters is plotted in Fig. 3. The equivalent circuit of a microstrip is shown in the inset. Inductance  $L$  and capacitance  $C$  per unit length are extracted from the measured scattering parameters. The variation of the permeability (complex) in the vicinity of FMR causes a significant drop of inductance  $L$ , while nearly no changes on capacitance  $C$  are observed.

In Fig. 4, it is demonstrated that the propagation wavelength  $\lambda$  of #A is shortened for frequencies up to 2.8 GHz ( $P_A$  in Fig. 4) as compared to #Ref. At 1 GHz, the wavelength of #A is reduced by 60% to about 4.4 cm. By increasing the aspect ratio of

FM prisms to 40 : 1, i.e., #B, the shortening of the wavelength continues up to 3.4 GHz ( $P_B$  in Fig. 4) due to the higher FMR frequency. However, below FMR, a higher aspect ratio implies a lower effective permeability  $\mu_{effc}$ , which results in a smaller wavelength reduction, as shown in Fig. 4 (#B). Above frequencies 2.9 and 3.4 GHz, the propagation wavelengths in #A and #B become longer than that in #Ref., respectively, due to the large variation of the effective permeability  $\mu_{effc}$  in the vicinity of the FMR frequency. Consequently, large wavelength reduction at high frequency relies on the FM materials with high FMR frequency that can be achieved by means of the micro-patterning of FM film (see Fig. 2).

Potential applications of using NiFe ferromagnetic microstrip devices are the band-stop filter and quarter wavelength microstrip lines. The stopband frequency is related to materials properties, e.g., ferromagnetic resonance frequency, and is fairly independent of the propagating wavelengths. This fact facilitates the miniaturization of devices. Furthermore, due to the dependence of the FMR frequency on the applied external dc magnetic field [see (1)], FM films can be utilized to design tunable stopband filters by varying the center stopband frequency. On the other hand, the length of the “so-called” quarter-wavelength microstrip lines is designed to be equal to one quarter of the propagation wavelength at a desired frequency. Therefore, applying ferromagnetic films, which consequently leads to a shorter propagation wavelength (see Fig. 4), offers further possibilities to minimize the on-chip design of quarter-wavelength microstrip lines.

#### IV. CONCLUSION

Microstrips with electroplated NiFe films has been integrated on silicon substrate using a fully IC-compatible process. High attenuation of about 19 dB/cm and large wavelength reduction of about 60% have been obtained for a 2-mm-long strip device. By micropatterning of the NiFe films into large aspect ratio prisms, center bandstop frequency rises up to 3.9 GHz.

#### ACKNOWLEDGMENT

The authors would like to thank the technical staffs at DIMES, Delft University of Technology, for their support on device processing and K. Attenborough, H. van Heren, J. Lambregts, and OnStream MST B.V. for the deposition of the NiFe films.

#### REFERENCES

- [1] G. A. Prinz and J. J. Krebs, “Molecular beam epitaxial growth of single-crystal Fe films on GaAs,” *Appl. Phys. Lett.*, vol. 39, pp. 397–399, Sept. 1981.
- [2] E. Schloemann, R. Tustison, J. Weissman, H. J. van Hook, and T. Varitimatos, “Epitaxial Fe films on GaAs for hybrid semiconductor-magnetic memories,” *J. Appl. Phys.*, vol. 63, pp. 3140–3142, Apr. 1988.
- [3] V. S. Liau, T. Wong, W. Stacey, S. Ali, and E. Schloemann, “Tunable band-stop filter based on epitaxial Fe film on GaAs,” in *IEEE MTT-S Dig.*, June 1991, pp. 957–960.
- [4] N. Cramer, D. Lucic, R. E. Camley, and Z. Celinski, “High attenuation tunable microwave notch filters utilizing ferromagnetic resonance,” *J. Appl. Phys.*, vol. 87, pp. 6911–6913, May 2000.
- [5] A. L. Adenot, O. Acher, T. Taffary, P. Queffelec, and G. Tanne, “Tunable Microstrip device controlled by a weak magnetic field using ferromagnetic laminations,” *J. Appl. Phys.*, vol. 87, pp. 6914–6916, May 2000.
- [6] S. Ikeda, T. Sato, A. Ohshiro, K. Yamasawa, and T. Sakuma, “A thin film type magnetic/dielectric hybrid transmission-line with a large wavelength shortening,” *IEEE Trans. Magn.*, vol. 37, pp. 2903–2905, July 2001.
- [7] B. C. Webb, M. E. Re, C. V. Jahnes, and M. A. Russak, “High-frequency permeability of laminated and unlaminated, narrow, thin-film magnetic strips,” *J. Appl. Phys.*, vol. 69, pp. 5611–5615, Apr. 1991.
- [8] W. P. Jayasekara, J. A. Bain, and M. H. Kryder, “High frequency initial permeability of NiFe and FeAlN,” *IEEE Trans. Magn.*, vol. 34, pp. 1438–1440, July 1998.
- [9] Y. Hsu, R. Fontana, M. Williams, P. Kasiraj, E. Lee, and J. McCord, “High frequency high field permeability of patterned  $\text{Ni}_{80}\text{Fe}_{20}$  and  $\text{Ni}_{45}\text{Fe}_{55}$  thin films,” *J. Appl. Phys.*, vol. 89, pp. 6808–6810, June 2001.
- [10] B. Lax and K. J. Button, *Microwave Ferrites and Ferrimagnetics*. New York: McGraw-Hill, 1962, pp. 145–219, 297–322.
- [11] R. I. Joseph and E. Schloemann, “Demagnetizing field in nonellipsoidal bodies,” *J. Appl. Phys.*, vol. 36, pp. 1579–1593, May 1965.
- [12] A. Aharoni, “Demagnetizing factors for rectangular ferromagnetic prisms,” *J. Appl. Phys.*, vol. 83, pp. 3432–3434, Mar. 1998.